

Selective successional transport of bacterial populations from rooted agricultural topsoil to deeper layers upon extreme precipitation events

Lu Zhang^a, Katharina Lehmann^b, Kai Uwe Totsche^b, Tillmann Lueders^{a, *}

^a Helmholtz Zentrum München, Institute of Groundwater Ecology, Neuherberg, Germany

^b Friedrich Schiller University Jena, Institute of Geosciences, Department of Hydrogeology, Jena, Germany

ARTICLE INFO

Keywords:

Natural rain
Artificial rain
Preferential flow
Seepage water
Soil bacterial communities

ABSTRACT

Substantial amounts of organic matter are mobilized from upper soil layers during extreme precipitation events. This results in considerable fluxes of carbon from plant-associated topsoil to deeper mineral soil and to groundwater. Microbes constitute an important part of this mobile organic matter (MOM) pool. Previous work has shown that specific bacteria associated with the rhizosphere of decaying maize roots were selectively transported with seepage water upon snowmelt in winter. However, effective mechanisms of mobilization and also possible distinctions to microbial transport for living root systems remain poorly understood. In the present study, bacteria in seepage water were sampled from lysimeters at an experimental maize field after extreme rain events in summer. We show that a distinctive subset of rhizoplane-associated bacterial populations was mobilized after summer rain, especially including abundant members of the *Bacteroidetes*, representing a microbial conduit for fresh plant-derived carbon inputs into deeper soil layers. Marked distinctions of seepage communities were not observed between lysimeters with a different relative contribution of preferential vs. matrix flow. Time-resolved analyses of seepage water during an artificial rain event revealed temporal patterns in the mobilization of certain lineages, with members of the *Chitinophagaceae*, *Sphingomonadaceae*, and *Bradyrhizobiaceae* preferentially mobilized in early and late seepage fractions, and members of the candidate phyla *Parcubacteria* and *Microgenomates* mobilized mostly in intermediate fractions. While average bacterial cell counts were at $\sim 10^7 \text{ ml}^{-1}$ in seepage water, the recovery of amended fluorescently labeled cells of *Arthrobacter globiformis* was low (0.2–0.6%) over seepage events. Still, mobilized bacteria clearly have the potential to influence bacterial activities and communities in subsoils. These findings demonstrate that dynamic hydraulic events must be considered for a better understanding of the connectivities between microbial populations and communities in soil, as well as of the links between distinct carbon pools over depth.

1. Introduction

Soil is the largest terrestrial reservoir of organic carbon, playing an essential role in global carbon sequestration (Lal, 2004). A primary source of soil organic matter (SOM) is provided by plants (Kögel-Knabner, 2002), which largely determine the distribution of OM (Jobbágy and Jackson, 2000). Transport of OM from topsoil to deeper soil layers with seepage water is a main component of carbon fluxes in soil, representing a significant contribution of fresh inputs of OM to subsoil and even to groundwater (Rumpel and Kögel-Knabner, 2011; Küsel et al., 2016).

Mobile organic matter in soil consists mostly of dissolved and colloidal organic carbon, including biocolloids like bacteria, fungi and their fragments (Totsche et al., 2007; Lehmann et al., 2018). The mechanisms of release and transport of such biocolloids and larger organic particles from the topsoil to subsoil are complex and poorly understood so far. They are highly influenced by dynamic environmental conditions like fluctuations in soil moisture, soil gas and temperature (Or et al., 2007). The soil pore network structure is a main controlling factor as a path for these fluxes, especially with the presence of macro- and biopores favoring the preferential and pronounced transport of OM (Jacobsen et al., 1997; Lægdsmand et al., 1999) and microorganisms

* Corresponding author. Institute of Groundwater Ecology, Helmholtz Zentrum München (GmbH), German Research Centre for Environmental Health, Ingolstädter Landstr. 1, 85764, Neuherberg, Germany.

Email address: tillmann.lueders@helmholtz-muenchen.de (T. Lueders)

(Bundt et al., 2001; Wang et al., 2013; Dibbern et al., 2014). The mobilization of viable microbes from topsoil mediated by preferential flow could also act as an important influx of biodiversity to subsoils, where the translocated microbes may significantly contribute to local microbial activities (Kieft et al., 1998; Jaesche et al., 2006; Küsel et al., 2016).

The importance of understanding bacterial mobility and transport mechanisms in soil has been increasingly recognized, mostly connected to the input of potential pathogens to groundwater (Bradford et al., 2013). In soil, bacteria either move actively (Sen, 2011), or are mobilized passively by advection after release to the mobile water phase (Wang et al., 2013), via nematodes (Knox et al., 2004), or along growing plant roots (Feeney et al., 2006) and fungal hyphae (Simon et al., 2015). Substantial amounts of suspended materials including bacterial biomass can be transported vertically from topsoil (Totsche et al., 2007; Lehmann et al., 2018), especially triggered by weather events producing large amounts of seepage, such as snowmelt or strong precipitation (Dibbern et al., 2014). Numerous column studies have been conducted to address how the transport of pathogenic bacteria amended to soil is affected by various physical, chemical and biological factors (Bradford et al., 2013). Distinct features, such as cellular shape (Weiss et al., 1995), hydrophobicity (Kim et al., 2009) surface charge (Bolster et al., 2009), and bacterial interactions (Stump et al., 2011) were found to influence bacterial detachment and transport behavior. However, while central aspects of the transport of selected bacterial strains in soil have been intensively investigated, our understanding of the release and transport of complex indigenous microbiota in natural soils remains limited.

We have previously addressed this knowledge gap by characterizing natural bacterial communities mobilized with seepage water after snowmelt in late winter on an experimental maize field in Germany (Dibbern et al., 2014). The findings suggested that preferential flow along root channels played an important role in the transport of topsoil bacteria to deeper soil layers, and specific subsets of bacteria associated with decaying roots were selectively mobilized. However, these first insights did not address the potential impacts of more pronounced precipitation events and variability of soil moisture on living root systems in summer. In the present study, we hypothesize that (i) distinct subsets of root-associated bacterial populations will be selectively mobilized and transported to deeper soil layers along living root channels in summer; and (ii) a differential contribution of effective flow paths, i.e. preferential vs. matrix flow, during seepage events should be reflected in dynamics of transported microbiota. To address this, we conducted seepage water sampling after natural and artificial extreme rain events in late summer. Via direct time-resolved sampling, we characterized mobile organic matter (MOM), related physicochemical parameters as well as mobilized complex microbiota throughout the seepage process and compared them to the surrounding soil- and root-associated microbiomes. Furthermore, we used fluorescently labeled viable cells of a bacterial strain characteristic of the site as a tracer, to quantify their mobilization and transport behavior during seepage events.

2. Materials and methods

2.1. Field site and lysimeters

The agricultural field was located in Holtensen, near the city of Göttingen (Germany). The area has a temperate climate, with a mean annual temperature of 7.9°C and a mean annual precipitation of 651 mm^y⁻¹ (1981–2010; Deutscher Wetterdienst, 2017; aggregated). The mean monthly precipitation (1981–2010, Göttingen weather station, 167 MAMSL; source: Deutscher Wetterdienst, 2017, aggregated) ranges between 39 and 66 mm (minima in February, April, October,

and maxima in June). Thresholds for extreme precipitation events were determined by rarity (99th percentile; cf. Beniston and Stephenson (2004)) and were at 16.6 mm d⁻¹ for summer (April–September) and at 22.0 mm d⁻¹ for winter (October–March). The dominant soil types are Cambisols (Braunerden), Luvisols (Parabraunerden) and stagnic Luvisols (Pseudogley) (IUSS Working Group WRB, 2007). The albic horizon typically found for these soils is not detectable, due to the long-term agricultural management with intensive tillage. Two plough layers were found at 20 and 30 cm below surface, with strong compaction below the second plough layer. Further details on chemical and physical soil properties can be found elsewhere (Kramer et al., 2012; Dibbern et al., 2014).

A long-term field experimental for tracing rhizosphere vs. detritusphere-derived carbon into the soil food web was established in May 2012, with 12 experimental plots (5×5 m) with three treatments (maize rooted, maize-litter-amended and fallow soil, Loepmann et al., 2016a, b). All plots with lysimeters used here were planted with maize since 2012. Tension-supported lysimeters (KL2-100, UMS, Munich, Germany) were installed directly below the plough horizon (35 cm depth) and below the main rooted zone (65 cm depth). To do so, a horizontal chute (40 cm width, 40 cm length, 25 cm height) was excavated via a hydraulic pit. The lysimeters were fully connected to the undisturbed soil overburden by a load compensation plate. A specifically designed, small-sized lysimeter setup was chosen to sample naturally low concentrated mobile particles (mineral and organic components, aggregates, biocolloids) up to a size of 10–250 μm (Totsche et al., 2018), which percolate from undisturbed soil. The lysimeters were composed of a stainless-steel ring (diameter: 30 cm; height: 10 cm) filled with inert glass beads (size/diameter: 2.0–2.5 mm) and a porous silicon carbide suction plate (SiC320; pore size of ~20 μm, air entry point of 100 hPa, less resistance to flow, diameter 32 cm, thickness 1 cm; UMS) at the bottom. Suction was applied and regulated via a vacuum controller (VS-twin, UMS) by using the prevailing soil water potential that was constantly measured with a tensiometer (T8, UMS) installed at 35 cm depth. While the porous plate was used to apply the suction to the system, the glass-bead layer served two purposes: It supported the undisturbed soil overburden and it acted as a “retention volume” for larger suspended particles and aggregates that may be released from the soil. Without the glass-bead layer, these materials would have resulted in filter clogging and rapid malfunction of the lysimeter system.

2.2. Sampling after a natural rain event

An extreme rainfall event of 30.2 mm occurred on 11.09.2012, followed by several successive precipitation events (0.2–0.4 mm; Fig. S1a) over the next days. Precipitation was measured with an iMETOS 2 weather station (Pessl Instruments, Weiz, Austria). The volumetric water content and soil temperature were measured with sensors (5TM, Decagon Devices, Pullman, USA) installed at 48 cm (n = 5) and 58 cm (n = 5) below soil surface in the hydraulic pit. Two pairs of co-localized lysimeters (35 cm and 65 cm depth) were investigated in two different plots, coded with A and B (L35A, L65A and L35B, L65B), which were ~15 m apart. On 19.09.2012, a further 2.8 mm rain event occurred before the actual sampling. Directly before sampling, empty sterilized glass bottles were installed to collect seepage water from the four lysimeters. Fresh seepage water was sampled within 24 h. Immediately after retrieval, seepage water was filtered for bacterial analyses (0.2 μm, Corning, New York, USA). Filters with retained microbial biomass were frozen at -20 °C until further processing (~3–6 months). For each 24-h water sample, DNA was extracted in duplicate from two sectioned filter quarters. In addition, subsamples were taken for physicochemical water analysis. On the same day, depth-resolved composite

soil samples were taken as described previously (Kramer et al., 2012; Dibbern et al., 2014) from the lysimeter plots. Furthermore, two live root balls were extracted from each plot. All soil and root samples were frozen and stored at -20°C until further analyses. Rhizosphere (Rh) and rhizoplane (Rp) samples were obtained as previously described (Dibbern et al., 2014). All bulk soil, rhizosphere and rhizoplane samples were obtained and processed in biological triplicates, whereas water samples were processed in biological duplicates due to volume restrictions.

2.3. Artificial rain experiment

To investigate the mobilization and transport of bacterial populations from topsoil under controlled experimental conditions, an artificial rain experiment was conducted in September 2014. The artificial rain experiment was set up for six lysimeters, all installed at 35 cm depth, but located in different replicate plots planted with maize, coded with A, B, C and D. Defined spikes of fluorescently labeled bacterial cells were amended to the topsoil of four lysimeters (L35A, L35B, LC, LD). Further two lysimeters (LE, LF) were intended as controls without cell amendment. We used *Arthrobacter globiformis* (DSM, 20124) obtained from the DSMZ (Braunschweig, Germany) as amendment. This strain is closely related to abundant *Arthrobacter* populations previously detected in both the rhizosphere (Dibbern et al., 2014; Zhang and Lueders, 2017) and detritusphere (Kramer et al., 2016) of the investigated soil. Cultures of *A. globiformis* were grown in liquid DSMZ medium 53 (*Corynebacterium* agar) for 24 h at 30°C . Before staining, cells were harvested by centrifugation at 3345 rcf for 15 min, washed twice with $1\times$ PBS buffer, and resuspended in 60 ml $1\times$ PBS. Thereafter, the cells were labeled with a fluorescent protein stain, CFDA/SE (5-(and-6)-carboxyfluorescein diacetate, succinimidyl ester; Life Technologies, Inc.), which has been shown to uniformly stain bacterial cells for up to five months, with no apparent influence on cell viability or transport behavior (Fuller et al., 2000, 2001). The staining was performed following a procedure modified from Fuller et al. (2000). Cell suspensions were evenly distributed to 1.5-ml Eppendorf tubes. Three μl of CFDA/SE (50 mM in dimethyl sulfoxide) were then added to 1.5 ml cell suspension to a final concentration of $100\mu\text{M}$. Cells were incubated on a thermomixer (Eppendorf, Germany) at 450 rpm for approximately 50 min, with temperature cycled between 25°C and 39°C over five cycles. Afterwards, cells were harvested by centrifugation at 10,000 rcf for 10 min, washed three times with $1\times$ PBS buffer, and resuspended in 200 ml $1\times$ PBS, evenly distributed to four 50-ml Falcon tubes. For quantification, $100\mu\text{l}$ of these cell suspensions were removed and measured using flow cytometry as described (Zhang and Lueders, 2017), with minor modifications. Cells were counted from 10^4 -, 10^5 - and 10^6 -fold dilutions generated in 10-fold dilution series prior to analysis. Flow-count fluorospheres (Beckman Coulter, Germany) were used as quantification standards (bead concentration: $1026\mu\text{l}^{-1}$).

The artificial rain water was composed of ultrapure, degassed water (Milli-Q[®]; Integral System, Merck, Darmstadt, Germany; equipped with a $0.22\text{-}\mu\text{m}$ membrane filter) amended with the following salts: 6.86 mg l^{-1} NaNO_3 (Carl Roth, Karlsruhe, Germany), 1.64 mg l^{-1} KHCO_3 (Carl Roth) and 33.97 mg l^{-1} $\text{CaSO}_4\times 2\text{ H}_2\text{O}$ (VWR, Darmstadt, Germany). As non-reactive tracer, 2 mM KBr were added for determination of water flow regimes, resulting in a Br^- concentration of 151 mg l^{-1} . The total electrical conductivity was $335\mu\text{S cm}^{-1}$ and the pH was 6.1. Although utmost cleanliness was applied during all procedures, the artificial rain water could not be handled or applied under sterile conditions. We discuss this below.

Two days before the artificial rain experiment in September 2014, two 2.9- and 4.5-mm rain events occurred, respectively (Fig. S1). Two rainfall simulator units (emc, Erfurt, Germany) were used to generate extreme but constant sprinkling irrigation following the principle of a Boyle-Mariotte bottle. Irrigation occurred via a network of 50 cannulas, $\sim 50\text{ cm}$ above the surface was applied at a uniform rate of 8 mm h^{-1} over $\sim 8\text{ h}$ per lysimeter ($50\times 50\text{ cm}$). This artificial irrigation of 64 mm represented an extreme rain event (16 l per 8 h). CFDA/SE-stained cells of *A. globiformis* were prepared in $1\times$ PBS buffer $\sim 48\text{ h}$ before amendment and transported to the field under cooling. One hour after the artificial rain started, 50 ml of cell suspension were amended to the topsoil above each of four lysimeters (L35A, L35B, LC, LD). Two other lysimeters (LE, LF), intended as controls, did not receive bacterial amendments. Cell suspensions were first transferred to a sterile 50-ml syringe and injected to topsoil above the lysimeters at $\sim 2\text{ cm}$ depth at ten random spots.

Seepage from the individual lysimeters was collected with sterilized glass bottles. For each sampling, bottles were exchanged and samples were collected when approximately $> 250\text{ ml}$ seepage water had accumulated, which was the minimum amount required for all downstream analyses. However, seepage water collection was only successful for two of the lysimeters with bacterial amendment (LC and LD). Seepage water did not accumulate in the two other lysimeters with bacterial amendment and in the two control lysimeters. Sampling was continued until no more seepage water was received, which lasted $\sim 27\text{ h}$ for LC and $\sim 23\text{ h}$ for LD. In the end, six time-resolved seepage water samples were collected for LC, and seven for LD, respectively. At least half of each collected sample was immediately filtered and stored for nucleic acid extraction as described above. Furthermore, 10 ml of each seepage water sample were fixed with glutardialdehyde (2.5% final conc.) for cell counting and stored at 4°C . Next to the lysimeters, bulk soil, rhizosphere and rhizoplane samples were again obtained as above. All bulk soil, rhizosphere and rhizoplane samples were processed in biological triplicates, whereas water samples were analyzed in duplicates due to volume restrictions.

2.4. Physicochemical analyses of seepage water

Electrical conductivity (EC) and pH of all seepage water samples were determined with field probes (Cond 197i, Sentix 41; WTW, Weilheim, Germany). Seepage water analyses included dissolved (DOC) and total organic carbon (TOC), measured by catalytic high-temperature combustion and non-dispersive infrared (NDIR) detection (multi N/C 2100S; Analytik Jena, Jena, Germany). DOC samples were filtered with $0.45\mu\text{m}$ PES syringe filters (Supor, Pall, Port Washington, USA). Total inorganic carbon (TIC) was measured by acidification with 10% phosphoric acid and NDIR-detection (same device). Sulfate, nitrate, and bromide were quantified by ion chromatography (IC 20, Dionex, Sunnyvale, USA). Turbidity was determined by UV-Vis spectroscopy (Cary 50 Conc, Varian, Darmstadt, Germany) as spectral absorption at 860 nm and converted to formazine attenuation units (FAU). The hydrodynamic diameter as well as the zeta potential (Nano ZS) were measured by dynamic light scattering (DLS; Nano ZS, Malvern Instruments, Worcester-shire, UK).

2.5. Molecular analyses

Total DNA from the filters, the soil samples (bulk and rhizosphere) and the root fragments was extracted as previously described (Dibbern et al., 2014) with minor modifications: sectioned filter quarters, $\sim 0.4\text{ g}$ soil (ww) and $\sim 0.5\text{ g}$ roots (ww) were used. Extracted nucleic acids were dissolved in $80\mu\text{l}$ EB buffer (Qiagen GmbH, Hilden, Germany).

DNA extraction was done for duplicate filter quarters and triplicate soil and rhizoplane samples. Bacterial community structure was first analyzed by 16S rRNA gene-targeted terminal restriction fragment length polymorphism (T-RFLP) fingerprinting as described (Dibbern et al., 2014; Zhang and Lueders, 2017). Then, 454 amplicon sequencing was performed for all water samples and duplicate soil and rhizoplane samples. For the natural rain event, sequencing was conducted using bacterial primers Ba27f/519r and Titanium chemistry as reported previously (Pilloni et al., 2012). Amplicons from the artificial rain experiment samples were generated using FLX + chemistry and bacterial primers Ba27f/907r as described more recently (Zhang and Lueders, 2017). Sequencing was done by IMG/M Laboratories (Munich, Germany). Raw reads obtained from both procedures were then demultiplexed and trimmed as described (Pilloni et al., 2012; Zhang and Lueders, 2017), and processed and classified using the SILVAngs data analysis platform (Quast et al., 2013). All sequencing raw data has been deposited with the NCBI sequence read archive under the SRA accession number SRP103676.

2.6. Cell counting of seepage water samples

Prior to cell counting of the fixed seepage water samples via flow cytometry, glutardialdehyde was removed by centrifugation of the samples at 18,000 rcf for 10 min and resuspending the cell pellets in 1×PBS buffer. Afterwards, density gradient centrifugation was performed to remove remaining soil particles (Grösbacher et al., 2016). For this, 1.5 ml of each sample was placed on top of 5 ml Nycodenz gradient solution (1.3g ml⁻¹; Axis-Shield Poc, Oslo, Norway) in 10 ml ultra-centrifugation tubes cooled to 4 °C. Samples were then centrifuged at 15,500 rcf and 4 °C in a swinging bucket rotor SW 40 Ti (Beckman Coulter, Germany) for 1 h. Thereafter, the top second and third 1-cm gradient fractions containing the purified cells were collected. Samples were diluted five-fold in 1×PBS buffer prior to analysis. Counting of the CFDA/SE-stained cells recovered in seepage water was performed as described above, but internal standard bead concentration was 992 μl⁻¹. For total cell counts in seepage water, samples were first stained with 1×SYBR Green I (Molecular Probes, Germany) for 10 min in the dark prior to measurements (Zhang and Lueders, 2017).

2.7. Statistical analysis

Bacterial community structures obtained from different seepage water samples, bulk soil, rhizosphere and rhizoplane samples were compared using principal component analysis (PCA), using both T-RFLP

fingerprinting and amplicon sequencing data sets. The relative abundances of OTUs were arcsin transformed ($\arcsin\sqrt{\cdot}$) prior to analyses (Ramette, 2007). PCA was performed using the function 'rda' from the package 'vegan' (Oksanen et al., 2017) in R (R Development Core Team, 2013). Pearson correlation coefficients were computed for relations between TOC and total cell counts of the time-resolved seepage water fractions in the artificial rain experiment, also in R.

3. Results

3.1. Seepage water and bacteria after a natural rain event

Fresh seepage water was first sampled within 24 h after a natural rain event of ~30 mm in late summer 2012 (~51 per lysimeter). Seepage water was taken in duplicates from two pairs of lysimeters located at 35 and 65 cm depth. The mean soil temperature was 15 °C at an air temperature of 14.5 °C on the sampling day. The mean volumetric water content (19.09.2012: 48 cm: 23 ± 1 vol%, 58 cm: 25 ± 1 vol%) was significant lower than the mean annual water content of the soil (2010–2012; 48 cm: 26 ± 3 vol%, 58 cm: 29 ± 3 vol%). The two sampled lysimeter plots (LA and LB) showed different seepage water characteristics over depth (Table 1). Lysimeter plot A produced a larger seepage volume at 65 cm, while OC, EC, nitrate, and sulfate concentrations decreased with depth. In contrast, lysimeter plot B showed an inverse trend, with a larger seepage volume collected at 35 cm, and higher concentrations of OC, anions and slightly higher EC at greater depth.

Bacterial communities in seepage water were first compared to those in respective soil and root samples using principal component analysis (PCA) based on both T-RFLP and sequencing data sets. The spatial ordination of distinct samples in PCA plots was mirrored for both data sets (Fig. 1). Seepage water samples were clearly separated from the bulk soil communities, especially along PC1, which seemed to be influenced mostly by compartments. Rhizoplane bacterial communities were further discriminated from the rhizosphere and bulk soil communities, and were placed closer to the seepage water samples along PC1 in both plots. The PC2s seemed to be mostly influenced by depth, which separated rhizoplane samples from rhizosphere, bulk soil and water samples at different depths. In general, replicated fingerprints and sequencing libraries were highly comparable, except that the fingerprints of bacterial communities in seepage water from the two 35 cm lysimeters appeared more variable along PC2.

Sequencing suggested that the bacterial taxa representative for seepage water were affiliated to the *Bacteroidetes* (*Chitinophagaceae*, *Cytophagaceae*, *Flavobacteriaceae* and *Sphingobacteriaceae*), and also the *Al-*

Table 1

Seepage water volume and hydrochemical parameters of the water samples taken after the natural rain event in September 2012. Duplicate lysimeters (A & B) were sampled at 35 and 65 cm depth each.

Lysimeter	Seepage volume	pH	EC	Nitrate	Sulfate
	l	-	μS cm ⁻¹	mg l ⁻¹	mg l ⁻¹
L35A	0.18	7.1	148	8.58	5.20
L65A	0.42	7.0	72	1.96	1.70
L35B	0.32	7.2	152	1.60	2.88
L65B	0.18	7.3	167	7.49	4.37
	TOC	DOC (< 0.45 μm)	POC (> 0.45 μm)	Hydrodynamic diameter	Zeta potential
	mg l ⁻¹	mg l ⁻¹	mg l ⁻¹	nm	mV
L35A	94.74	2.92	91.82	1165	-16.6
L65A	16.88	2.67	14.21	<i>p</i>	-
L35B	7.09	2.61	4.48	<i>p</i>	-
L65B	18.47	3.33	15.14	982	-16.4

p – Polydispersity of the sample resulted in no clear hydrodynamic diameter and zeta potential measurement.

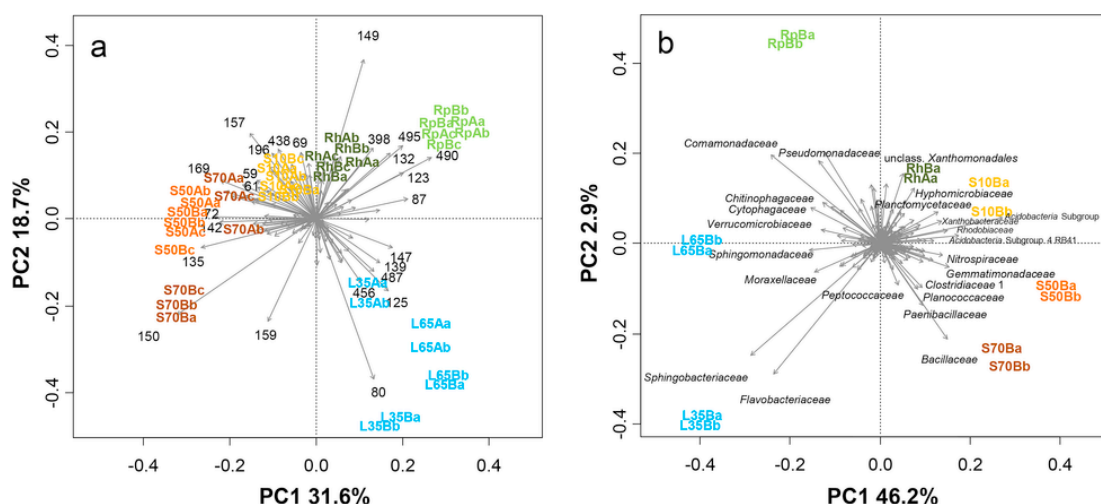


Fig. 1. PCA biplots of T-RFLP (a) and amplicon sequencing (b) data sets of samples obtained after a natural rain event. Seepage water was sampled from two pairs of lysimeters installed at 35 cm and 65 cm depth (LA35, LA65 and LB35, LB65). S10, S50, S70: bulk soil samples from 0 to 10, 40–50 and 60–70 cm depth; Rh: rhizosphere; Rp: rhizoplane. Sample codes are shown in bold and in colors according to sampled compartments. Biological duplicates (a,b) of water samples and triplicates (a,b,c) of soil and rhizoplane samples were first analyzed by T-RFLP (A), whereas duplicates (a,b) of water, soil and root samples from only one of the two lysimeters (LB) per depth were subject to amplicon sequencing (B). T-RFs (A) and taxa (B) are denoted by grey arrows, with selected discriminant T-RFs or taxa labeled or named, respectively. (For interpretation of the references to color in this figure legend, the reader is referred to the Web version of this article.)

phaproteobacteria (*Spingomonadaceae*), *Gammaproteobacteria* (*Moraxellaceae*) and *Verrucomicrobia* (*Verrucomicrobiaceae*), as shown in Fig. 1b. Reads related to the *Comamonadaceae* (*Betaproteobacteria*) seemed to be characteristic for both the 65 cm lysimeter water samples and rhizoplane samples. Another lineage that appeared associated to rhizoplane samples was the *Pseudomonadaceae* (*Gammaproteobacteria*). Reads affiliated to unclassified *Xanthomonadales* (*Gammaproteobacteria*) and *Hyphomicrobiaceae* (*Alphaproteobacteria*) were more important in rhizosphere and 10 cm bulk soil samples. In contrast, taxa found characteristic for bulk soil mostly belonged to the *Firmicutes* (*Bacillaceae*, *Clostridiaceae*, *Paenibacillaceae*, *Peptococcaceae* and *Planococcaceae*), the *Acidobacteria* (Subgroup 4 RB41 and Subgroup 6), the *Alphaproteobacteria* (*Rhodobiaceae* and *Xanthobacteraceae*) and also the *Gemmatimonadetes* (*Gemmatimonadaceae*), *Nitrospirae* (*Nitrospiraceae*) and *Planctomycetes* (*Planctomycetaceae*). Members of the *Firmicutes* were especially characteristic for bulk soil at 60–70 cm depth.

The comparison of taxon-level community composition of overall sequencing libraries substantiated these pronounced differences between the seepage water and bulk soil communities, as well as over depth (Fig. 2). Reads of the *Flavobacteriaceae*, *Spingobacteriaceae* and *Bacillaceae* were much more abundant in water at a depth of 35 cm (18, 21 and 6%) than at 65 cm (4, 2 and 3%). Families that appeared more frequent in seepage water at 65 cm included the *Spingomonadaceae* (8 vs. 4%), *Comamonadaceae* (15 vs. 2%), *Oxalobacteraceae* (5 vs. 1%) and *Pseudomonadaceae* (8 vs. 1%). Some of the taxa abundant in seepage water were also frequent on the rhizoplane, i.e. the *Chitinophagaceae* (L35: 4%, L65: 3%, Rp: 6%), *Cytophagaceae* (L35: 3%, L65: 4%, Rp: 6%), *Comamonadaceae* (Rp: 11%), *Oxalobacteraceae* (Rp: 4%) and *Pseudomonadaceae* (Rp: 6%). All of them were very low in relative abundance in bulk soil. Other taxa found in seepage water and hardly observed in bulk soil included the *Flavobacteriaceae*, *Spingobacteriaceae* and *Spingomonadaceae*. In stark contrast, reads within the *Acidobacteria* and *Chloroflexi* were abundant in bulk soil and in the rhizosphere, but almost absent in seepage samples. Also, *Firmicutes* were predominant in rhizosphere and bulk soils, especially in soils at 40–50 cm and 60–70 cm depth, but were clearly lower in relative abundance in seepage waters (L35: 13%, L65: 8%, S50: 21%, S70: 38%).

3.2. Artificial rain experiment

An artificial rain experiment was applied over six lysimeters in Sept. 2014, but seepage water was only obtained for two of the lysimeter plots with bacterial amendment (LC and LD). Seepage water sampling at 35 cm depth for LC and LD lasted ~27 h and ~23 h, respectively, until no more seepage water appeared. Six time-resolved water samples were collected for LC (T1-6; ~210 ml average vol.) and seven samples were obtained for LD (T1-6, ~250 ml average vol.; T7 contained only 22 ml of water and was omitted from molecular work). From the total applied volume, i.e. 16 l per lysimeter, 1.25 l and 1.51 l (8–9%) were recovered. The pH of the seepage water was nearly constant after an initial increase for both lysimeters, slightly higher than the original pH of the artificial rain water (pH 6.1) and generally lower in LD (Fig. 3a). Similarly, the EC values increased to a maximum after ~0.5 l of total seepage water volume (LC: 430 $\mu\text{S cm}^{-1}$; LD: 390 $\mu\text{S cm}^{-1}$; Fig. 3a), followed by a subsequent decrease to around the original EC of the artificial rain water (335 $\mu\text{S cm}^{-1}$). The breakthrough curves of bromide as conservative tracer were distinct for the two lysimeters (Fig. 3b). The curve for LC was characterized by increasing concentrations and a peak of 101 mg l^{-1} after 0.5 l seepage was produced, while similarly high concentrations of bromide immediately appeared in LD (0.2 l, 110 mg l^{-1}). Notable declines were observed after 4–5 fractions of seepage water (> 1 l in total) had been collected. The Br^- concentration of the artificial rain (151 mg l^{-1}) was never reached in both lysimeters. In total, only ~4–6% of the amended bromide mass was recovered in seepage waters of LC and LD, respectively.

The fluxes of TOC (and DOC) also differed between both lysimeters (Fig. 3c). LC showed an initial OC concentration of 18 mg l^{-1} , which then decreased to a constant level of ~10 mg l^{-1} . The contribution of particular organic carbon (POC, > 0.45 μm) to TOC was initially high for LC (~43%), but then decreased with flow time). Initial TOC concentrations were slightly higher in LD (~21 mg l^{-1}), decreased transiently in fractions 3 and 4, but then increased to final concentrations around ~27 mg l^{-1} . Similarly, the POC content was initially much higher for

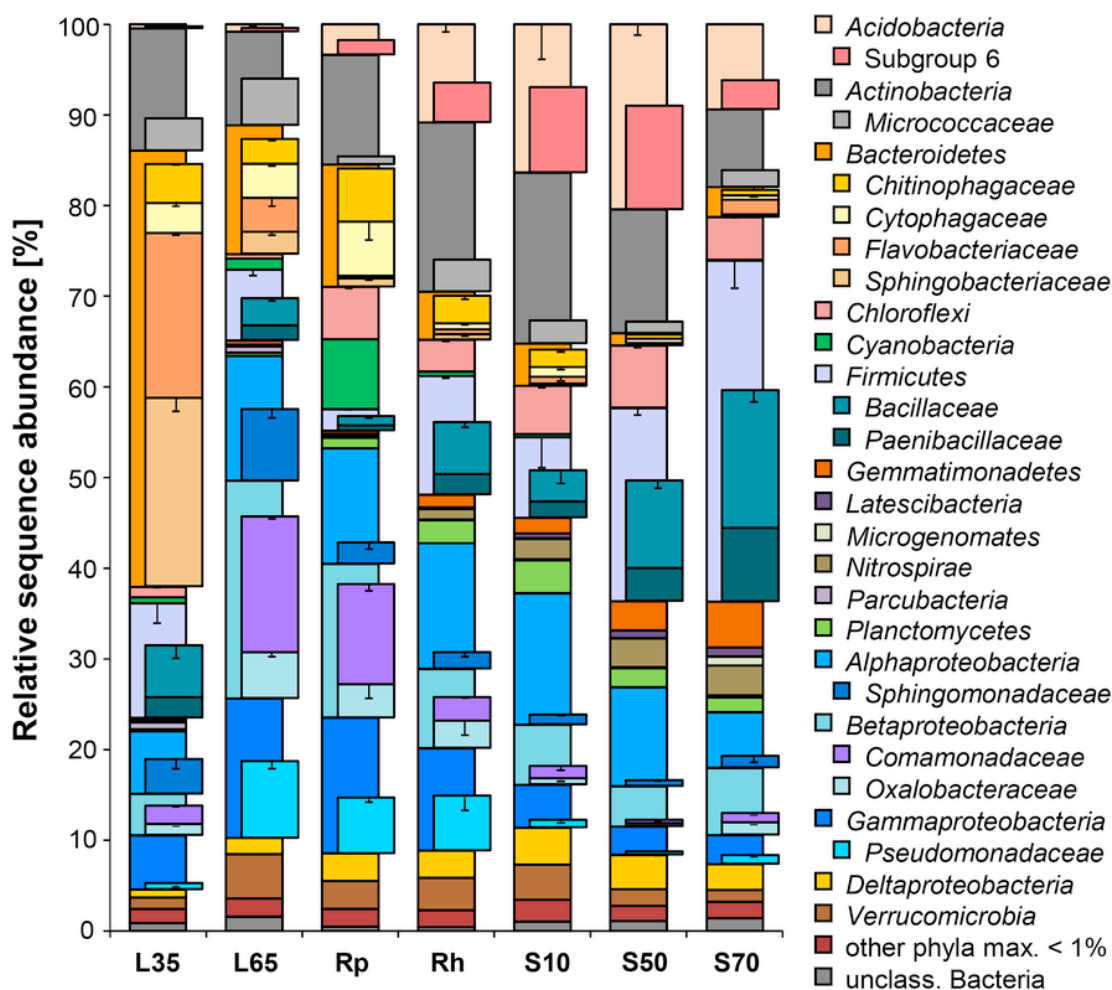


Fig. 2. Relative sequence abundance for bacterial taxa obtained by amplicon sequencing of samples taken during a natural rain event. All phyla with average relative sequence abundance >1% in at least one of the compartments are shown, as well as *Microgenomates* and *Parcubacteria* (<1%, mentioned in text). Error bars (negative only) represent standard error ($n = 2$) of duplicate sequencing libraries. Selected abundant sub-phylum taxa are highlighted. Sample codes are as in Fig. 1.

LD (69% of TOC), decreased to ~20%, and then increased again towards final seepage water fractions. Total cell counts fluctuated around $\sim 10^7$ cells ml^{-1} of seepage water (Fig. 3d). Total cell counts and TOC export appeared correlated for LD (Pearson's $r = 0.85$).

3.3. Mobilized bacteria after artificial rain experiment

Bacterial communities recovered in successive seepage water fractions from the two lysimeters were analyzed by T-RFLP fingerprinting and amplicon sequencing. The spatial ordination of distinct samples in PCA biplots was again consistent for both data sets (Fig. 4). The PC1s largely separated the seepage water communities recovered from LC and LD. Interestingly, the PC2s arranged the samples from LC and LD in comparable time-resolved patterns. The first water samples (LCT1 & LDT1) were always well-separated from subsequent samples. In both the fingerprinting and sequencing data sets, bacterial communities for early and late time points of seepage water recovery appeared somewhat related, while they were more distinct from the samples for intermediate fractions (LCT2-5, LDT3-5). The bacterial communities mobilized in LD generally showed a greater variation over time.

The PCA biplots helped to identify bacterial taxa characteristic for the different time points of seepage water collection in the two lysimeters (Fig. 4b). While members of the *Bradyrhizobiaceae* (*Alphaproteobacteria*) seemed to be especially characteristic for initial seepage water

samples, members of two candidate phyla, *Microgenomates* and *Parcubacteria*, were enriched in intermediate seepage fractions. Furthermore, members of the *Flavobacteriaceae*, *Sphingobacteriaceae* (both within the *Bacteroidetes*), *Planctomycetaceae* (*Planctomycetes*) and others appeared associated with intermediate water samples of LC, while the *Chitinophagaceae* (*Bacteroidetes*), *Nitrospiraceae* (*Nitrospirae*), *Comamonadaceae* (*Betaproteobacteria*) and others occurred especially in respective fractions of LD.

Overall taxon-level community dynamics generally substantiated the marked distinctions between water and soil bacterial communities, as well as shifts in mobilized populations in seepage water over time (Fig. 5). Members of the *Bacteroidetes*, the *Gammaproteobacteria* and the candidate phyla *Microgenomates*, *Parcubacteria*, SM2F11 and TM6, were of enriched abundance in seepage water samples, and much less abundant or almost absent in soil. In contrast, the *Acidobacteria*, *Actinobacteria*, *Chloroflexi*, *Firmicutes* and *Gemmatimonadetes*, although abundant in bulk soil, were much less frequently detected in seepage water. The rhizoplane, rhizosphere and bulk soil samples showed highly similar overall communities between the two lysimeters, while the rhizoplane samples again appeared generally more similar to the seepage water samples (Fig. 5). Consistent variations in relative sequence abundance during seepage water collection were observed for several bacterial taxa in both lysimeters. For example, mobilized *Chitinophagaceae*, while being generally more abundant in LD, were always more abundant in fractions 1 and 6 of both lysimeters. The alphaproteobacterial *Sphin-*

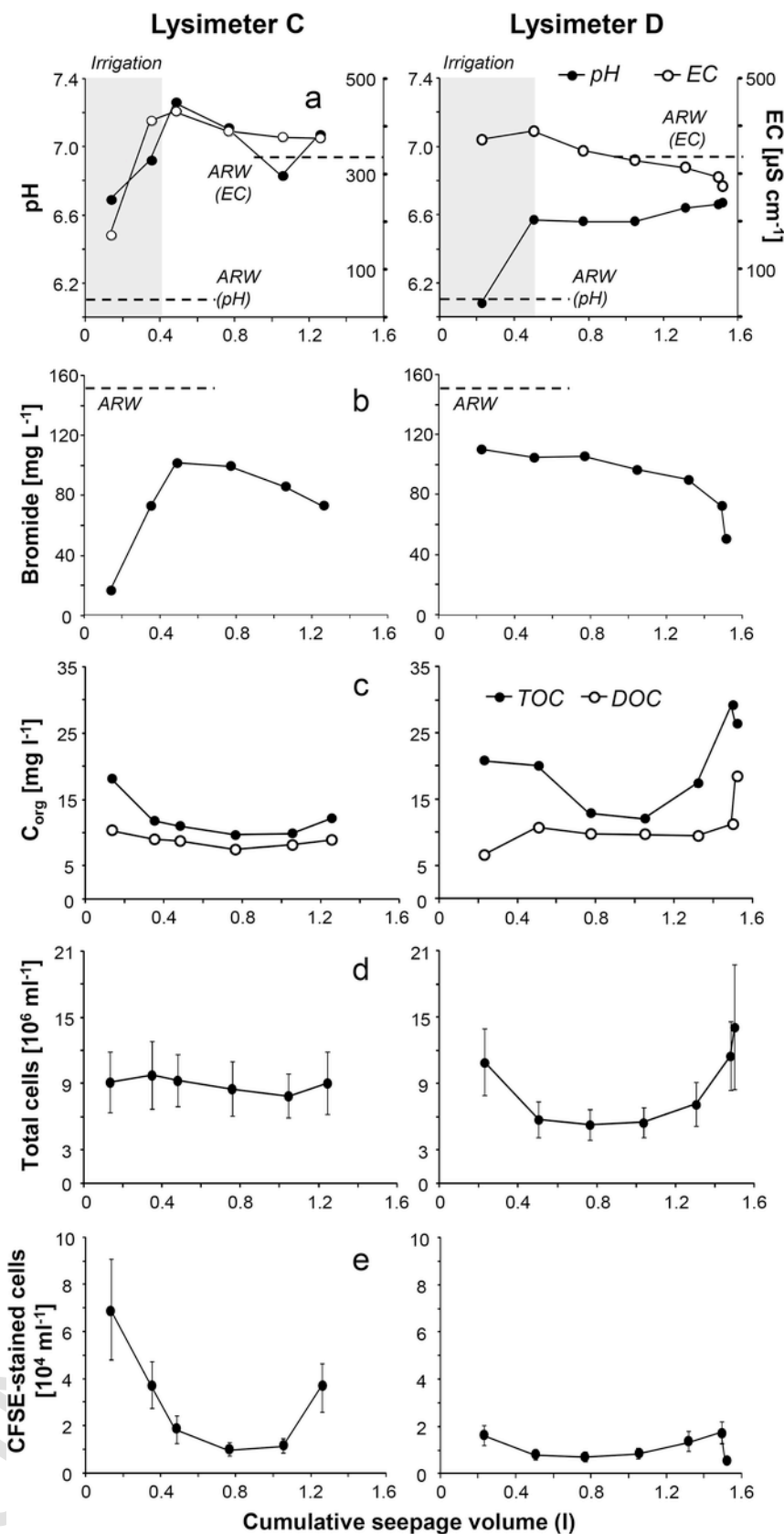


Fig. 3. Temporal profiles of pH and EC (a), bromide (b), TOC and DOC (c), total bacterial cells (d) and CFSE-stained cells (e) detected in successive seepage water fractions from LC and LD during the artificial rain experiment. pH, EC and bromide concentration in the original artificial rain water (ARW) are indicated by dashed lines. Error bars represent standard error ($n = 2$) of duplicate measurements in (d) and (e), and are too small for visualization in (c, internal). Single measurements were conducted for (a) and (b).

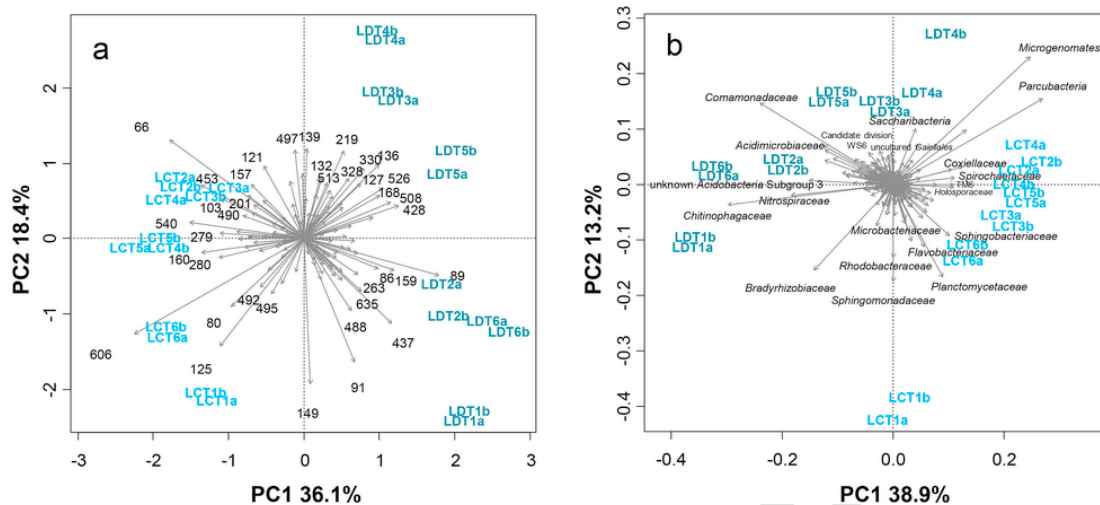


Fig. 4. PCA biplots of bacterial communities in seepage water sampled during the artificial rain experiment based on T-RFLP (a) and amplicon sequencing (b) data. Water samples were collected from two lysimeters (LC and LD). All samples were subjected to fingerprinting and sequencing in biological duplicates. T-RFs (a) and taxa (b) are denoted by grey arrows, with selected relevant T-RFs or taxa labeled or named, respectively.

gomonadaceae and *Bradyrhizobiaceae* showed a similar pattern, same as members of the *Comamonadaceae*, the latter only for LD. In contrast, reads within the *Microgenomates* and *Parcubacteria* showed a general increase in abundance between fractions 1 and 4 in both lysimeters, followed by slight decreases in relative abundance until the end of the seepage event. Members of the *Gammaproteobacteria* (*Coxiellaceae*, *Legionellaceae*) also steadily increased and were most abundant in intermediate water fractions collected from both lysimeters.

Live fluorescently labeled cells of *A. globiformis* were amended to topsoil above LC and LD during the artificial rain experiment at a concentration of $\sim 2.8 \times 10^9$ cells ml^{-1} (50 ml per lysimeter). This corresponded to an amendment of $\sim 6.2 \times 10^7$ cells per g_{dw} of topsoil (assuming a more or less even distribution throughout the first 2 cm of soil), and thus $\sim 3\%$ of the indigenous bacterial biomass (previously quantified at $\sim 2.1 \times 10^9$ cells per g_{dw} ; Dibbern et al. (2014)). The breakthrough curves of CFDA/SE-stained cells recovered in seepage water were much lower in concentration, in a range of $10^4 - 10^5$ cells ml^{-1} (Fig. 3e). The concentration of recovered labeled bacterial cells was always lower in LD seepage water than in LC, but fluxes in both lysimeters seemed to follow a similar pattern of slightly increased concentrations at the start and towards the end of the seepage process (similar as for TOC and total cells). Corrected for the total amount of bromide tracer retained in seepage water, about ~ 0.6 and $\sim 0.2\%$ of the amended *A. globiformis* cells were recovered in LC and LD, respectively.

4. Discussion

In this study we traced MOM, mainly in terms of TOC, DOC and bacterial populations, translocated from maize-rooted topsoil to deeper horizons after extreme rain events in late summer. To the best of our knowledge, this is the first study to specifically address the nature of mobilized seepage microbiota after summer rain, including a time-resolved sampling during the artificial rain event. The difficulty of reliable seepage water collection in the field was illustrated by a considerable variability of seepage behavior between lysimeters during both events. The fact that the analysis of a fully replicated set of lysimeters (and also strain amendment controls) was thus prevented, clearly limits the generalizations possible from our findings.

After the natural rain event, the release and transport of MOM in LA seemed to be influenced by preferential flow over depth, as indicated by a higher seepage volume and lower organic content and EC at

65 cm depth. In contrast, LB appeared to be comparably more influenced by matrix flow, with lower seepage volumes but increasing solute concentrations over depth. Both illustrates the importance of local heterogeneities in hydraulic connectivity and differences in soil pore structure for seepage water formation (Cey et al., 2009), even for the relatively homogeneous and regularly tilled agricultural soil at the site (Kramer et al., 2012; Scharroba et al., 2012). The variability between lysimeters was even more apparent during the artificial rain experiment, where only two of the six installations produced seepage water at all. We attribute this to the occurrence of diverted flow along the two compacted plow layers (at 20 and 30 cm depth; Kramer et al. (2012)), where a large share of the precipitation may have bypassed the lysimeters. Moreover, by assuming a mean soil porosity of $0.41 \text{ cm}^3 \text{ cm}^{-3}$ for the topsoil (Kramer et al., 2012), the estimated pore volume of 351 (141 by assuming 25 vol% water content) in the upper 35 cm soil monoliths emphasizes that unsaturated flow conditions prevailed throughout the artificial rain event of 16l. A significant share of the irrigated water may simply have contributed to a recharge of the soil water storage capacity at the end of the dry summer. However, the rapid arrival and high initial concentrations of the Br^- tracer, especially in LD, also points to the activation of preferential flow paths (Jacobsen et al., 1997; Cey et al., 2009) along secondary macropores, most likely earthworm burrows or root-channels. Nevertheless, the lower initial concentrations and slightly delayed arrival of Br^- suggested a relatively larger contribution of matrix flow and resided soil water to seepage water in LC. Potentially, this should also be reflected in mobilized microbiota of both lysimeters.

4.1. Mobilized bacterial populations in summer seepage

In contrast to the above assumption, systematic differences between the microbiota mobilized in LA & LD (comparably less matrix flow) and LB & LC (more matrix flow) were not observed. Rather, as previously observed for decaying roots after snowmelt in winter (Dibbern et al., 2014), mobilized bacterial communities always appeared highly influenced by rhizoplane communities, suggesting an important role of mobilization via seepage flow along live root channels in summer. Moreover, many dominant lineages mobilized in winter were consistently observed also in summer, such as members of the *Sphingobacteriaceae* (*Bacteroidetes*), the *Sphingomonadaceae* and *Bradyrhizobiaceae* (*Alphaproteobacteria*), the *Comamonadaceae* (*Betaproteobacteria*) and the

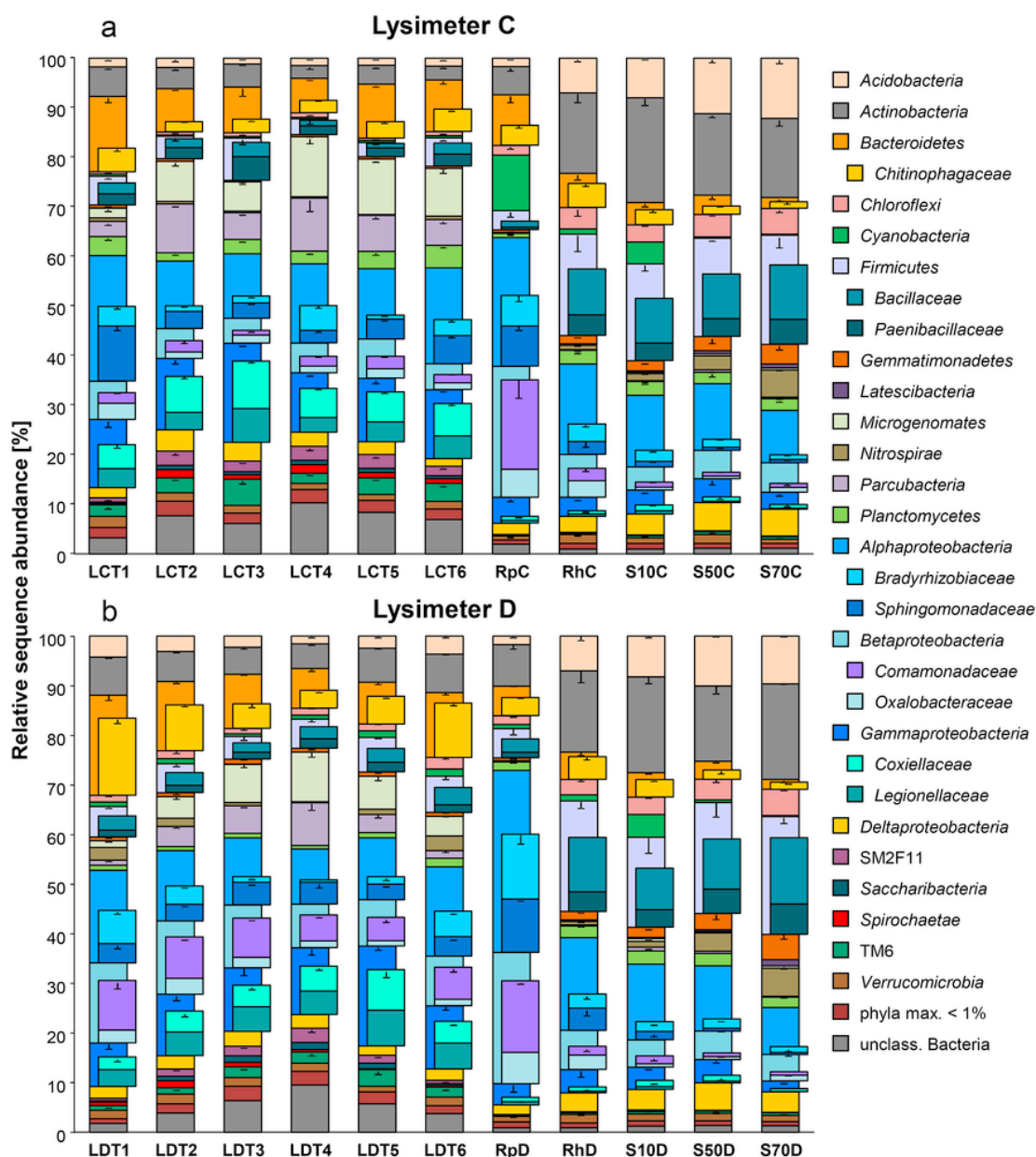


Fig. 5. Relative sequence abundance for bacterial taxa obtained by amplicon sequencing of successive seepage water and soil samples during the artificial rain experiment. Error bars (negative only) represent standard error ($n = 2$) of duplicate sequencing libraries. Selected abundant sub-phyllum taxa are highlighted. Sample codes and other details are as in Figs. 1 and 4.

Legionellaceae (Gammaproteobacteria). In summer, however, members of the *Bacteroidetes* (*Flavobacteriaceae* and *Sphingobacteriaceae*) appeared much more enriched in seepage water than in winter. Members of both families have been previously reported as typical maize rhizosphere bacteria (Li et al., 2014; Yang et al., 2017). Their abundant detection in seepage water after extreme rain suggests a notable ‘flushing effect’ along root channels, despite living roots interact closely with associated microbes by releasing exudates, mucilage and border cells to increase the root-microbe bond (Haichar et al., 2014) and counteract rhizopore water flow (Ghestem et al., 2011).

Interestingly, members of the *Parcubacteria* and *Microgenomates*, both belonging to the candidate phyla previously named OD1 and OP11 (Brown et al., 2015), consistently appeared enriched in successive seepage water samples during the artificial rain experiment. They were not abundant in previous winter seepage (Dibbern et al., 2014), but also detected in seepage water after natural rain, albeit at much

lower relative abundance (Fig. 2). Since both lineages belong to the ultra-small bacteria and can pass through $\sim 0.2\mu\text{m}$ membranes (Luef et al., 2015), we were at first concerned of whether they could have been introduced with the artificial rain water. Although this was indeed filtered through $0.22\mu\text{m}$ membranes, handling and application of the artificial rain water could not be realized under sterile conditions, which calls for a cautioning of respective conclusions. However, an ‘ex post’ test of water originating from the same Milli-Q machine produced cell counts as low as $\sim 10^2\text{ml}^{-1}$, approaching the detection limit of the cytometer. This was much lower than the $\sim 10^7\text{cells ml}^{-1}$ detected in seepage water after the artificial rain experiment, and thus could not have caused a contamination notable in seepage water sequencing libraries. Moreover, members of the *Parcubacteria* have been recently reported for several rhizosphere soils including that of maize (Correa-Galeote et al., 2016; Dawson et al., 2017). Therefore, our observation

that these lineages may be selectively mobilized from oxic rhizosphere systems with seepage water adds a new perspective to their potential origin in the subsurface, where they are currently considered to be rather characteristic for anoxic groundwater (Luef et al., 2015; Nelson and Stegen, 2015).

4.2. Dynamic nature of the artificial seepage event

A key finding of the present study was the dynamic nature of seepage water microbiota observed between successive fractions of the artificial rain experiment. Here, members of the *Chitinophagaceae*, *Sphingomonadaceae* and *Bradyrhizobiaceae* were amongst the populations with the most characteristic “early” and “late” patterns of mobilization. Since the respective water fractions also were lowest in EC, close to the respective conductivity of the artificial rain water, it can be speculated that the mobilization of these lineages was influenced by the comparably low ionic strength (Wang et al., 2013; Choi et al., 2017) of the artificial rain water. Higher concentrations of organic matter have also been reported to promote bacterial transport through soil (Jimenez-Sanchez et al., 2015), a characteristic also observed in early and late seepage water fractions. In contrast, members of the *Parcubacteria*, *Microgenomates* and the potentially pathogenic *Legionellaceae* were enriched in intermediate seepage fractions. Cellular parameters like hydrophobicity (Wan et al., 1994; Kim et al., 2009) or surface charge (Bolster et al., 2009) could have influenced their delayed mobilization behavior. The contribution of matrix flow could also have increased in intermediate seepage fractions, resulting in a sequential mobilization of microbes from the soil matrix. Irrespective of which mechanisms were ultimately controlling this distinct mobilization behavior of populations in seepage water, targeted transport experiments under controlled conditions with variable strain amendments will be necessary to further elucidate the possible regulators. In the present study, the consistent observation of such mobilization patterns between duplicate lysimeters demonstrates, that different overarching factors control the detachment and mobilization of specific populations within complex soil microbiota.

4.3. Low recovery of the amended *Arthrobacter globiformis*

A. globiformis cells were amended to the artificial rain experiment as a fluorescently labeled bacterial tracer. Members of this genus and closely related bacteria were identified as abundant and functionally relevant in rhizosphere and bulk soil of the investigated field site (Kramer et al., 2016; Zhang and Lueders, 2017). We are aware that a single bacterial strain will not reflect the full spectrum of conceivable transport behaviors effective for microbes at the site. Still, we believe this tracer can provide a first reference for quantifying bacterial efflux with seepage from topsoil.

Various other *Arthrobacter* strains have been used previously in bacterial transport experiments, mostly in laboratory studies (Gannon et al., 1991; Wan et al., 1994). *Arthrobacter* spp. typically feature lysine as diamino acids in the cell wall and are characterized by a growth cycle in which cells are rod-shaped in young cultures and coccoid in older cultures (Jones and Keddie, 2006). A low recovery of the *A. globiformis* amendment of only ~0.2–~0.6% was observed in our artificial rain experiment. Still, considering maximal recovery rates of ~8% reported for *Arthrobacter* cells transported through 5 cm columns of a loam soil (Gannon et al., 1991), our recovery of up to ~0.6% at 35 cm depth of a natural Cambisol/Luvisol was not exceedingly low. The compacted plough layer present at the field site could also have obstructed the transport of microbes to deeper soil layers. Still, our results support the idea that the application of labeled microbial strains isolated from or closely related to indigenous microbes can provide valuable insights on subsurface bacterial transport and mobility (Fuller et al., 2004).

5. Conclusions

Our results provide primary insights on how the mobility of specific soil microbiota upon extreme precipitation events can link distinct metacommunities across soil compartments. We also uncover a marked dynamic nature of MOM and microbiota mobilized between successive fractions of seepage water. This adds a new perspective to our understanding of the heterogeneity and physical separation of microbial habitats in soil as being a major driver of soil microbial diversity (Zhou et al., 2002; Or et al., 2007; Carson et al., 2010). If occasional hydraulic events are considered, this should allow for sufficient connectivities between microbial habitats in soil macro- and micropores to counteract spatial isolation as evolutionary mechanisms potentially effective during dryer periods. The observed high intra-event dynamics of mobilized microbial populations may even be an important determinant for subsoil microbial community composition and dynamics, as well as their activity in soil carbon cycling.

For selected populations originating from topsoil, i.e. for the observed *Legionellaceae*, their mobilization during extreme precipitation events and their fate in deeper soil and in groundwater is not without relevance for the spreading of potential pathogens. Numerous studies have demonstrated the leaching and spreading of pathogens from agricultural soils to groundwater, especially under the application of manure (Bradford et al., 2013; Oliver and Heathwaite, 2013). Also for other lineages, such as the *Parcubacteria* and *Microgenomates* observed in intermediate seepage fractions, a better mechanistic understanding of their mobilization and transport behavior will be crucial for making predictions on their impact on subsoils and groundwater under scenarios of an increasing intensity and frequency of extreme precipitation (Baker et al., 2011; Min et al., 2011). To this end, we believe that our study can provide important first cues, as well as that it can inspire further research on soil microbiomes mobilized in seepage water.

Acknowledgements

This study was funded by grants of the DFG (Deutsche Forschungsgemeinschaft) within the Research Unit “Carbon flow in belowground food webs assessed by isotope tracers” (FOR 918) to T.L. and K.U.T. Further support was provided by the Helmholtz Society and the FSU Jena. We like to thank Andreas Schmalwasser (Institute of Geoscience, FSU Jena) for organization and implementation of the field experiments. We are grateful to Nina Weber (Helmholtz Zentrum München) for help with cytometric cell counting. Furthermore, we thank Anton Hartmann (Helmholtz Zentrum München) for providing the bacterial strain used in this project.

Appendix A. Supplementary data

Supplementary data related to this article can be found at <https://doi.org/10.1016/j.soilbio.2018.06.012>.

References

- Baker, A., Tahani, D., Gardiner, C., Bristow, K.L., Greenhill, A.R., Warner, J., 2011. Groundwater seeps facilitate exposure to *Burkholderia pseudomallei*. *Applied and Environmental Microbiology* 77, 7243–7246.
- Beniston, M., Stephenson, D.B., 2004. Extreme climatic events and their evolution under changing climatic conditions. *Global and Planetary Change* 44, 1–9.
- Bolster, C.H., Haznedaroglu, B.Z., Walker, S.L., 2009. Diversity in cell properties and transport behavior among 12 different environmental *Escherichia coli* isolates. *Journal of Environmental Quality* 38, 465–472.
- Bradford, S.A., Morales, V.L., Zhang, W., Harvey, R.W., Packman, A.I., Mohanram, A., Wely, C., 2013. Transport and fate of microbial pathogens in agricultural settings. *Critical Reviews in Environmental Science and Technology* 43, 775–893.

- Brown, C.T., Hug, L.A., Thomas, B.C., Sharon, I., Castelle, C.J., Singh, A., Wilkins, M.J., Wrighton, K.C., Williams, K.H., Banfield, J.F., 2015. Unusual biology across a group comprising more than 15% of domain bacteria. *Nature* 523, 208.
- Bundt, M., Widmer, F., Pesaro, M., Zeyer, J., Blaser, P., 2001. Preferential flow paths: biological 'hot spots' in soils. *Soil Biology and Biochemistry* 33, 729–738.
- Carson, J.K., Gonzalez-Quinones, V., Murphy, D.V., Hinz, C., Shaw, J.A., Gleeson, D.B., 2010. Low pore connectivity increases bacterial diversity in soil. *Applied and Environmental Microbiology* 76, 3936–3942.
- Cey, E.E., Rudolph, D.L., Passmore, J., 2009. Influence of macroporosity on preferential solute and colloid transport in unsaturated field soils. *Journal of Contaminant Hydrology* 107, 45–57.
- Choi, N.-C., Choi, J.-W., Kwon, K.-S., Lee, S.-G., Lee, S., 2017. Quantifying bacterial attachment and detachment using leaching solutions of various ionic strengths after bacterial pulse. *AMB Express* 7, 38.
- Correa-Galeote, D., Bedmar, E.J., Fernández-González, A.J., Fernández-López, M., Arone, G.J., 2016. Bacterial communities in the rhizosphere of amilaceous maize (*Zea mays* L.) as assessed by pyrosequencing. *Frontiers of Plant Science* 7, 1016.
- Dawson, W., Hör, J., Egert, M., van Kleunen, M., Pester, M., 2017. A small number of low-abundance bacteria dominate plant species-specific responses during rhizosphere colonization. *Frontiers in Microbiology* 8, 975.
- Dibbern, D., Schmalwasser, A., Lueders, T., Totsche, K.U., 2014. Selective transport of plant root-associated bacterial populations in agricultural soils upon snowmelt. *Soil Biology and Biochemistry* 69, 187–196.
- Feeney, D.S., Crawford, J.W., Daniell, T., Hallett, P.D., Nunan, N., Ritz, K., Rivers, M., Young, I.M., 2006. Three-dimensional microorganization of the soil-root-microbe system. *Microbial Ecology* 52, 151–158.
- Fuller, M.E., Mailloux, B.J., Streger, S.H., Hall, J.A., Zhang, P., Kovacic, W.P., Vainberg, S., Johnson, W.P., Onstott, T.C., DeFlaun, M.F., 2004. Application of a vital fluorescent staining method for simultaneous, near-real-time concentration monitoring of two bacterial strains in an Atlantic coastal plain aquifer in Oyster, Virginia. *Applied and Environmental Microbiology* 70, 1680–1687.
- Fuller, M.E., Mailloux, B.J., Zhang, P.F., Streger, S.H., Hall, J.A., Vainberg, S.N., Beavis, A.J., Johnson, W.P., Onstott, T.C., DeFlaun, M.F., 2001. Field-scale evaluation of CFDA/SE staining coupled with multiple detection methods for assessing the transport of bacteria in situ. *FEMS Microbiology Ecology* 37, 55–66.
- Fuller, M.E., Streger, S.H., Rothmel, R.K., Mailloux, B.J., Hall, J.A., Onstott, T.C., Fredrickson, J.K., Balkwill, D.L., DeFlaun, M.F., 2000. Development of a vital fluorescent staining method for monitoring bacterial transport in subsurface environments. *Applied and Environmental Microbiology* 66, 4486–4496.
- Gannon, J.T., Manilal, V.B., Alexander, M., 1991. Relationship between cell surface properties and transport of bacteria through soil. *Applied and Environmental Microbiology* 57, 190–193.
- Ghestem, M., Sidle, R.C., Stokes, A., 2011. The influence of plant root systems on subsurface flow: implications for slope stability. *BioScience* 61, 869–879.
- Grösbacher, M., Spicher, C., Bayer, A., Obst, M., Karwautz, C., Piloni, G., Wachsmann, M., Scherb, H., Griebler, C., 2016. Organic contamination versus mineral properties: competing selective forces shaping bacterial community assembly in aquifer sediments. *Aquatic Microbial Ecology* 76, 243–255.
- Haichar, F.e.Z., Santaella, C., Heulin, T., Achouak, W., 2014. Root exudates mediated interactions belowground. *Soil Biology and Biochemistry* 77, 69–80.
- IUSS Working Group WRB, 2007. World Reference Base for Soil Resources 2006, First Update 2007, World Soil Resources Reports No. 103. Food and Agriculture Organization of the United Nations, Rome, 97–107.
- Jacobsen, O.H., Moldrup, P., Larsen, C., Konnerup, L., Petersen, L.W., 1997. Particle transport in macropores of undisturbed soil columns. *Journal of Hydrology* 196, 185–203.
- Jaesche, P., Totsche, K.U., Kögel-Knabner, I., 2006. Transport and anaerobic biodegradation of propylene glycol in gravel-rich soil materials. *Journal of Contaminant Hydrology* 85, 271–286.
- Jimenez-Sanchez, C., Wick, L.Y., Cantos, M., Ortega-Calvo, J.-J., 2015. Impact of dissolved organic matter on bacterial tactic motility, attachment, and transport. *Environmental Science and Technology* 49, 4498–4505.
- Jobbágy, E.G., Jackson, R.B., 2000. The vertical distribution of soil organic carbon and its relation to climate and vegetation. *Ecological Applications* 10, 423–436.
- Jones, D., Keddle, R.M., 2006. The genus *Arthrobacter*. In: Dworkin, M., Falkow, S., Rosenberg, E., Schleifer, K.-H., Stackebrandt, E. (Eds.), *The Prokaryotes: Volume 3: Archaea. Bacteria: Firmicutes, Actinomycetes*. Springer New York, New York, NY, pp. 945–960.
- Kieft, T.L., Murphy, E.M., Haldeman, D.L., Amy, P.S., Bjornstad, B.N., McDonald, E.V., Ringelberg, D.B., White, D.C., Stair, J., Griffiths, R.P., Gsell, T.C., Holben, W.E., Boone, D.R., 1998. Microbial transport, survival, and succession in a sequence of buried sediments. *Microbial Ecology* 36, 336–348.
- Kim, H.N., Bradford, S.A., Walker, S.L., 2009. *Escherichia coli* O157:H7 transport in saturated porous media: role of solution chemistry and surface macromolecules. *Environmental Science and Technology* 43, 4340–4347.
- Knox, O.G., Killham, K., Artz, R.R., Mullins, C., Wilson, M., 2004. Effect of nematodes on rhizosphere colonization by seed-applied bacteria. *Applied and Environmental Microbiology* 70, 4666–4671.
- Kögel-Knabner, I., 2002. The macromolecular organic composition of plant and microbial residues as inputs to soil organic matter. *Soil Biology and Biochemistry* 34, 139–162.
- Kramer, S., Dibbern, D., Moll, J., Huenninghaus, M., Koller, R., Krueger, D., Marhan, S., Urlich, T., Wubet, T., Bonkowski, M., Buscot, F., Lueders, T., Kandeler, E., 2016. Resource partitioning between bacteria, fungi, and protists in the detritusphere of an agricultural soil. *Frontiers in Microbiology* 7, 1524.
- Kramer, S., Marhan, S., Ruess, L., Armbruster, W., Butenschoten, O., Haslswimmer, H., Kuzyakov, Y., Pausch, J., Scheunemann, N., Schoene, J., Schmalwasser, A., Totsche, K.U., Walker, F., Scheu, S., Kandeler, E., 2012. Carbon flow into microbial and fungal biomass as a basis for the belowground food web of agroecosystems. *Pedobiologia* 55, 111–119.
- Küsel, K., Totsche, K.U., Trumbore, S.E., Lehmann, R., Steinhäuser, C., Herrmann, M., 2016. How deep can surface signals be traced in the critical zone? Merging biodiversity with biogeochemistry research in a central German Muschelkalk landscape. *Frontiers of Earth Science* 4, 32.
- Lægdsmand, M., Villholth, K.G., Ullum, M., Jensen, K.H., 1999. Processes of colloid mobilization and transport in macroporous soil monoliths. *Geoderma* 93, 33–59.
- Lal, R., 2004. Soil carbon sequestration impacts on global climate change and food security. *Science* 304, 1623–1627.
- Lehmann, K., Schafer, S., Babin, D., Köhne, J.M., Schlüter, S., Smalla, K., Vogel, H.-J., Totsche, K.U., 2018. Selective transport and retention of organic matter and bacteria shapes initial pedogenesis in artificial soil - a two-layer column study. *Geoderma* 325, 37–48.
- Li, X., Rui, J., Mao, Y., Yannarell, A., Mackie, R., 2014. Dynamics of the bacterial community structure in the rhizosphere of a maize cultivar. *Soil Biology and Biochemistry* 68, 392–401.
- Loeppmann, S., Blagodatskaya, E., Pausch, J., Kuzyakov, Y., 2016a. Enzyme properties down the soil profile - a matter of substrate quality in rhizosphere and detritusphere. *Soil Biology and Biochemistry* 103, 274–283.
- Loeppmann, S., Blagodatskaya, E., Pausch, J., Kuzyakov, Y., 2016b. Substrate quality affects kinetics and catalytic efficiency of exo-enzymes in rhizosphere and detritusphere. *Soil Biology and Biochemistry* 92, 111–118.
- Luef, B., Frischkorn, K.R., Wrighton, K.C., Holman, H.-Y.N., Birarda, G., Thomas, B.C., Singh, A., Williams, K.H., Stegerist, C.E., Tringe, S.G., Downing, K.H., Comolli, L.R., Banfield, J.F., 2015. Diverse uncultivated ultra-small bacterial cells in groundwater. *Nature Communications* 6, 6372.
- Min, S.-K., Zhang, X., Zwiers, F.W., Hegerl, G.C., 2011. Human contribution to more-intense precipitation extremes. *Nature* 470, 378–381.
- Nelson, W., Stegen, J., 2015. The reduced genomes of *Parcubacteria* (OD1) contain signatures of a symbiotic lifestyle. *Frontiers in Microbiology* 6, 713.
- Oksanen, J., Blanchet, F.G., Friendly, M., Kindt, R., Legendre, P., McGinn, D., Minchin, P.R., O'Hara, R.B., Simpson, G.L., Solymos, P., Stevens, M.H.H., Szoecs, E., Wagner, H., 2017. *Vegan: community ecology package*. In: *Ordination Methods, Diversity Analysis and Other Functions for Community and Vegetation Ecologists*, R package version: 2.4–2 ed <https://cran.r-project.org/web/packages/vegan/>.
- Oliver, D.M., Heathwaite, L.A., 2013. Pathogen and nutrient transfer through and across agricultural soils. In: Laws, E.A. (Ed.), *Environmental Toxicology: Selected Entries from the Encyclopedia of Sustainability Science and Technology*. Springer New York, New York, NY, pp. 403–439.
- Or, D., Smets, B.F., Wraith, J.M., Dechesne, A., Friedman, S.P., 2007. Physical constraints affecting bacterial habitats and activity in unsaturated porous media - a review. *Advances in Water Resources* 30, 1505–1527.
- Piloni, G., Granitsiotis, M.S., Engel, M., Lueders, T., 2012. Testing the limits of 454 pyrotag sequencing: reproducibility, quantitative assessment and comparison to T-RFLP fingerprinting of aquifer microbes. *PLoS One* 7, e40467.
- Quast, C., Pruesse, E., Yilmaz, P., Gerken, J., Schweer, T., Yarza, P., Peplies, J., Glöckner, F.O., 2013. The SILVA ribosomal RNA gene database project: improved data processing and web-based tools. *Nucleic Acids Research* 41, D590–D596.
- R Development Core Team, 2013. *R: a Language and Environment for Statistical Computing*. R Foundation for Statistical Computing, Vienna, Austria <http://www.R-project.org>.
- Ramette, A., 2007. Multivariate analyses in microbial ecology. *FEMS Microbiology Ecology* 62, 142–160.
- Rumpel, C., Kögel-Knabner, I., 2011. Deep soil organic matter—a key but poorly understood component of terrestrial C cycle. *Plant and Soil* 338, 143–158.
- Scharroba, A., Dibbern, D., Hünninghaus, M., Kramer, S., Moll, J., Butenschoten, O., Bonkowski, M., Buscot, F., Kandeler, E., Koller, R., Krüger, D., Lueders, T., Scheu, S., Ruess, L., 2012. Effects of resource availability and quality on the structure of the micro-food web of an arable soil across depth. *Soil Biology and Biochemistry* 50, 1–11.
- Sen, T.K., 2011. Processes in pathogenic biocolloidal contaminants transport in saturated and unsaturated porous media: a review. *Water, Air, and Soil Pollution* 216, 239–256.
- Simon, A., Bindschedler, S., Job, D., Wick, L.Y., Filippidou, S., Kooli, W.M., Verrecchia, E.P., Junier, P., 2015. Exploiting the fungal highway: development of a novel tool for the in situ isolation of bacteria migrating along fungal mycelium. *FEMS Microbiology Ecology* 91, fiv116-fiv116.
- Stumpff, C., Lawrence, J.R., Hendry, M.J., Maloszewski, P., 2011. Transport and bacterial interactions of three bacterial strains in saturated column experiments. *Environmental Science and Technology* 45, 2116–2123.
- Totsche, K.U., Amelung, W., Gerzabek, M.H., Guggenberger, G., Klumpp, E., Knief, C., Lehdorff, E., Mikutta, R., Peth, S., Prechtel, A., Ray, N., Kögel-Knabner, I., 2018. Microaggregates in soils. *Journal of Plant Nutrition and Soil Science* 181, 104–136.
- Totsche, K.U., Jann, S., Kögel-Knabner, I., 2007. Single event-driven export of polycyclic aromatic hydrocarbons and suspended matter from coal tar-contaminated soil. *Vadose Zone Journal* 6, 233–243.

- Wan, J., Wilson, J.L., Kieft, T.L., 1994. Influence of the gas-water interface on transport of microorganisms through unsaturated porous media. *Applied and Environmental Microbiology* 60, 509–516.
- Wang, Y., Bradford, S.A., Šimůnek, J., 2013. Transport and fate of microorganisms in soils with preferential flow under different solution chemistry conditions. *Water Resources Research* 49, 2424–2436.
- Weiss, T.H., Mills, A.L., Hornberger, G.M., Herman, J.S., 1995. Effect of bacterial cell shape on transport of bacteria in porous media. *Environmental Science and Technology* 29, 1737–1740.
- Yang, Y., Wang, N., Guo, X., Zhang, Y., Ye, B., 2017. Comparative analysis of bacterial community structure in the rhizosphere of maize by high-throughput pyrosequencing. *PLoS One* 12, e0178425.
- Zhang, L., Lueders, T., 2017. Micropredator niche differentiation between bulk soil and rhizosphere of an agricultural soil depends on bacterial prey. *FEMS Microbiology Ecology* 93, fix103.
- Zhou, J., Xia, B., Treves, D.S., Wu, L.Y., Marsh, T.L., O'Neill, R.V., Palumbo, A.V., Tiedje, J.M., 2002. Spatial and resource factors influencing high microbial diversity in soil. *Applied and Environmental Microbiology* 68, 326–334.

UNCORRECTED PROOF